Journal of Organometallic Chemistry, 438 (1992) 371–384
Elsevier Sequoia S.A., Lausanne
JOM 22832

The synthesis and characterization of σ-bonded gold carbaborane compounds: *closo*-carbaboranes as good σ-donor ligands

Bruce D. Reid and Alan J. Welch
Department of Chemistry, University of Edinburgh, Edinburgh EH9 3JJ (UK)

(Received April 7, 1992)

Abstract

A series of σ-bonded phosphine and arsine gold carbaborane compounds, 1-R′-2-ER_3Au-1,2-*closo*-$C_2B_{10}H_{10}$ (R′ = CH_2OCH_3 or Ph, ER_3 = PPh_3, P(*o*-tol)$_3$, PCy_3, PEt_3 or $AsPh_3$) have been prepared by reaction between ER_3AuCl and Li[1-R′-1,2-*closo*-$C_2B_{10}H_{10}$] in Et_2O. Consideration of their ^{11}B NMR and (where appropriate) ^{31}P NMR chemical shifts implies that the *closo*-carbaborane ligands function as efficient electron donating groups. Comparison of the Au–C distance in 1-CH_2OCH_3-2-$AsPh_3$Au-1,2-*closo*-$C_2B_{10}H_{10}$ (**1e**) and $AsPh_3AuCH_3$ (**3**) suggests that the gold–carbon bond in the former is stronger, and this is supported by analysis of the results of molecular orbital calculations at the extended Hückel level on model compounds. *closo*-Carbaboranes bonded to metal atoms via a M–C bond are thereby shown to be good σ-donor ligands.

Introduction

In comparison to the profusion of transition metal *closo*-carbametallaboranes in which the metal atom is η-bonded to a (*nido*) carbaborane ligand (recently termed [1] class 1 carbametallaboranes), there are remarkably few examples of compounds in which the metal and (*closo*) carbaborane cage are linked by a 2c–2e bond (class 3 carbametallaboranes). A review of the literature [2] revealed that class 3 transition metal carbametallaboranes are only known for d^6 or greater metal configurations, with metal–ligand bonding predominantly via a cage carbon atom. Many of these compounds are, moreover, relatively unstable via cleavage of the metal–carbon bond, *e.g.*, 1-Ph-2-{CpFe(CO)$_2$}-1,2-*closo*-$C_2B_{10}H_{10}$ (Cp = η^5-C_5H_5) is stable in aromatic solvents [3] but degrades to [CpFe(CO)$_2$]$_2$ and 1-Ph-1,2-*closo*-$C_2B_{10}H_{11}$ in CH_2Cl_2 [4].

In 1970, Mitchell and Stone [5] reported class 3 carba-auraboranes of unusual stability, and suggested that this could be related to "the... electron-withdrawing influence of the carb(ab)orane group." This implies that the {Ph_3PAu} fragment to

---

Correspondence to: Dr. A.J. Welch.

which the carbaborane is bonded acts as an electron donating moiety, in contrast to current ideas [6] about the bonding capabilities of such a unit, the (occupied) valence *d* orbitals of which are low-lying.

In this paper, we report the synthesis and characterization of a wide range of class 3 phosphine and arsine gold carbaborane compounds, and present the results of spectroscopic, crystallographic, and theoretical studies which collectively suggest that an alternative description of a *closo*-carbaborane ligand, namely as an effective σ-donor, is more appropriate.

Experimental

Syntheses

All syntheses were carried out under dry, oxygen-free nitrogen by standard Schlenk line techniques, with some subsequent manipulations in the air. Unless otherwise stated, all solvents were dried and distilled under nitrogen, and then degassed just before use. NMR spectra (Table 1) were recorded at room temperature from $CDCl_3$ solutions on JEOL FX90Q (^{31}P-{^1H}) and Bruker WP200SY (^{11}B and ^1H) spectrometers. Chemical shifts are quoted relative to external 85% H_3PO_4 (^{31}P), $BF_3 \cdot OEt_2$ (^{11}B) and $SiMe_4$ (^1H). IR spectra were obtained as KBr pellets on a Perkin–Elmer 598 spectrophotometer. Microanalyses (Table 1) were performed by the departmental service. The starting materials PR_3AuCl [7], $AsPh_3AuCl$ [7], 1-Ph-1,2-*closo*-$C_2B_{10}H_{11}$ [8] and 1-CH_2OCH_3-1,2-*closo*-$C_2B_{10}H_{11}$ [9] were prepared as previously described or by modified versions thereof. $AsPh_3AuMe$ (**3**) was synthesized (yield 52%) by an analogous procedure to that previously reported for PPh_3AuMe [10].

*Synthesis of 1-CH_2OCH_3-2-{PPh_3Au}-1,2-*closoC$_2$B$_{10}$H$_{10}$ (**1a**). To a stirred solution of 0.100 g (0.53 mmol) of 1-CH_2OCH_3-1,2-*closo*-$C_2B_{10}H_{11}$ in sodium-dried diethyl ether (10 cm^3) at 0°C was added dropwise 0.45 cm^3 of a 1.4 *M* solution of LiMe in diethyl ether (0.63 mmol). The resulting solution was allowed to warm to room temperature and then added dropwise to a stirred suspension of 0.263 g (0.53 mmol) of PPh_3AuCl in diethyl ether (15 cm^3). The solution became pale orange and most of the solid dissolved. After stirring for 1 h the mixture was filtered and the filtrate evaporated *in vacuo*. Crystallization from CH_2Cl_2/hexane yielded 1-CH_2OCH_3-2-{PPh_3Au}-1,2-*closo*-$C_2B_{10}H_{10}$ (**1a**) as colourless crystals in 38% yield. IR ν_{max} at 2556 (B–H) cm^{-1}. Similarly were prepared colourless, crystalline 1-CH_2OCH_3-2-{P(*o*-tol)$_3$Au}-1,2-*closo*-$C_2B_{10}H_{10}$ (*o*-tol = C_6H_4Me-2) (**1b**) (37%), ν_{max} at 2575 cm^{-1}; 1-CH_2OCH_3-2-{PCy_3Au}-1,2-*closo*-$C_2B_{10}H_{10}$] (Cy = *cyclo*-C_6H_{11}) (**1c**) (32%), ν_{max} at 2565 cm^{-1}; 1-CH_2OCH_3-2-{PEt_3Au}-1,2-*closo*-$C_2B_{10}H_{10}$ (**1d**) (26%), ν_{max} at 2555 cm^{-1}; 1-CH_2OCH_3-2-{$AsPh_3Au$}-1,2-*closo*-$C_2B_{10}H_{10}$ (**1e**) (31%), ν_{max} at 2580 cm^{-1}; 1-Ph-2-{PPh_3Au}-1,2-*closo*-$C_2B_{10}H_{10}$ (**2a**) (37%), ν_{max} at 2562 cm^{-1}; 1-Ph-2-{P(*o*-tol)$_3$Au}-1,2-*closo*-$C_2B_{10}H_{10}$ (**2b**) (36%), ν_{max} at 2578 cm^{-1}; 1-Ph-2-{PCy_3Au}-1,2-*closo*-$C_2B_{10}H_{10}$ (**2c**) (31%), ν_{max} at 2568 cm^{-1}; 1-Ph-2-{$AsPh_3Au$}-1,2-*closo*-$C_2B_{10}H_{10}$ (**2e**) (38%), ν_{max} at 2582 cm^{-1}. In the case of **1d**, purification of the crude product by TLC (Kieselgel 60 F_{254}, CH_2Cl_2 eluant, pale orange band with $R_f = 0.9$) was necessary before crystallization.

*Reaction of **1e** with PPh_3.* To a stirred solution of **1e** (0.017 g, 0.026 mmol) in CH_2Cl_2 (5 cm^3) at room temperature was added dropwise a solution of PPh_3 (0.007 g, 0.026 mmol) in the same solvent (3 cm^3). After 2 h, solvent was removed

Table 1

Microanalytical [a] and NMR data

Complex	C (%)	H (%)	δ(^1H) (ppm)	δ(^{31}P) (ppm)	δ(^{11}B) (ppm)
1a	40.9(40.3)	4.68(4.84)	7.56–7.32 (m, 15H, C_5H_5) 3.89 (s, 2H, CH_2) 3.27 (s, 3H, CH_3)	38.63	−0.97(1B), −3.97(1B), −7.27(2B), −9.27(6B)
1b	43.6(43.8)	5.27(5.23)	7.77–6.73 (m, 12H, C_6H_4Me) 3.78 (s, 2H, CH_2) 3.12 (s, 3H, OCH_3) 2.67 (s, 9H, $C_6H_4CH_3$)	16.56	−1.49(1B), −3.95(1B), −7.35(2B), −9.68(6B)
1c	39.8(40.9)	7.28(7.47)	3.82 (s, 2H, CH_2O) 3.33 (s, 3H, CH_3) 2.14–1.21 (m, 33H, C_6H_{11})	55.60	−1.36(1B), −4.14(1B), −7.28(2B), −9.71(6B)
1d	23.2(23.9)	5.95(6.02)	3.82 (s, 2H, CH_2O) 3.32 (s, 3H, OCH_3) 1.73 (t, 22 Hz, 9H, CH_2CH_3) 1.22 (q, 22 Hz, 6H, CH_2CH_3)	37.20	−1.48(1B), −4.09(1B), −7.20(2B), −9.73(6B)
1e	38.3(38.6)	4.38(4.71)	7.56–7.46 (m, 15H, C_6H_5) 3.93 (s, 2H, CH_2) 3.31 (s, 3H, CH_3)	–	−1.34(1B), −4.01(1B), −7.28(2B) −8.78(6B)
2a	46.0(46.3)	4.46(4.60)	7.86–7.10 (m, C_6H_5)	38.63	−0.42(1B), −3.45(1B), −6.99(4B), −8.34(4B)
2b	48.3(47.0)	5.04(5.06)	7.72–6.62 (m, 17H, aryl) 2.35 (s, 9H, $C_6H_4CH_3$)	16.56	−0.63(1B), −3.24(1B), −6.92(4B), −8.43(4B)
2c	44.8(44.4)	6.95(6.89)	7.81–7.15 (m, 5H, C_6H_5) 1.84–1.15 (m, 33H, C_6H_{11})	55.19	−0.60(1B), −3.54(1B) −6.98(4B), −8.45(4B)
2e	43.2(43.3)	4.19(4.34)	7.90–7.12 (m, C_6H_5)	–	−0.27(1B), −3.43(1B), −6.95(4B), −8.55(4B)
3	44.2(44.0)	3.76(3.50)	7.46–7.38 (m, 15H, C_6H_5) 0.63 (s, 3H, CH_3)	–	–

[a] Calculated values in parentheses.

in vacuo and Et_2O (5 cm^3) added. The resultant solid and solution were separated by filtration. Microanalysis of the solid was consistent with the formulation $C_{18}H_{15}As$. Solvent was removed from the filtrate and the resultant pale yellow solid shown to be **1a** by ^{31}P NMR spectroscopy.

X-Ray crystallography

All measurements were made on an Enraf–Nonius CAD4 diffractometer operating with graphite-monochromated Mo-K_α X-radiation, λ(bar) = 0.71069 Å, and equipped with a ULT-1 low temperature device (nitrogen cooling stream). Suitable

Table 2

Crystallographic data and details of data collection and structure solution and refinement

	Compound **1e**	Compound **3**
Formula	$C_{22}H_{30}B_{10}AsAuO \cdot CH_2Cl_2$	$C_{19}H_{18}AsAu$
M	775.40	518.24
Crystal system	Triclinic	Monoclinic
Space group	$P\bar{1}$	$P2_1/c$
a (Å)	9.6664(22)	9.0168(24)
b (Å)	12.706(8)	11.3808(21)
c (Å)	12.787(4)	17.413(4)
α (°)	93.78(4)	90
β (°)	97.282(23)	104.563(18)
γ (°)	102.32(4)	90
V (Å^3)	1514.8(12)	1729.4(7)
Z	2	4
D (g cm^{-3})	1.700	1.990
μ (cm^{-1})	61.24	103.78
F(000) (e)	748	976
θ range (setting) (°)	9–15	12–14
θ range (data collection) (°)	1–25	1–25
T	185 ± 1 K	291 ± 1 K
h range	$0 \rightarrow 11$	$0 \rightarrow 10$
k range	$-15 \rightarrow 15$	$0 \rightarrow 13$
l range	$-15 \rightarrow 15$	$-20 \rightarrow 20$
ω scan speeds (° min^{-1})	0.92–2.35	0.92–2.35
Data measured	5713	3463
Data observed	4814	2459
Criterion for observed	$F \geq 2.0\sigma(F)$	$F \geq 2.0\sigma(F)$
Data collection time (h)	120	76
H atom thermal parameter (Å^2)	0.093(9) (non-cage) 0.083(11) (cage)	0.102(10)
g	0.001280	0.000260
R	0.0524	0.0462
R_w	0.0670	0.0431
S	1.132	1.165
No. variables	374	191
Maximum shift/e.s.d.	0.50 [a]	0.01
Maximum residue (e Å^{-3})	2.29 [b]	0.92
Minimum residue (e Å^{-3})	−3.32	−1.06

[a] Disordered solvate. [b] Close to Au.

crystals of both **1e** and **3** were obtained by slow diffusion of hexane into CH_2Cl_2 solutions at −30°C. Unit cell parameters and orientation matrices were obtained by the least-squares refinement of the setting angles of 25 strong, high angle reflections. Data collection was by ω–2θ scans in 96 steps (ω scan width $0.8 + 0.34 \tan \theta$) at variable scan speeds. For **1e**, neither significant crystal decay nor movement was noted, but the crystal of **3** suffered a 30% decay in the average net intensity of two periodically remeasured check reflections and data were scaled accordingly. Data were corrected for Lorentz and polarization effects CADABS [11],

Table 3

Coordinates of refined atoms in **1e**

	x	y	z	U_{eq}
Au	0.17560(3)	0.48470(2)	0.26374(2)	0.0398(2)
As	0.00550(9)	0.33080(6)	0.17702(6)	0.0385(4)
C(11)	0.0461(9)	0.2846(6)	0.0385(6)	0.041(4)
C(12)	0.1316(10)	0.3605(8)	−0.0130(8)	0.055(5)
C(13)	0.1684(10)	0.3294(10)	−0.1087(8)	0.065(6)
C(14)	0.1256(11)	0.2250(9)	−0.1521(8)	0.069(7)
C(15)	0.0351(14)	0.1484(9)	−0.0993(8)	0.071(7)
C(16)	−0.0024(11)	0.1810(8)	−0.0047(8)	0.059(6)
C(21)	−0.0113(9)	0.2033(6)	0.2518(6)	0.039(4)
C(22)	0.1115(11)	0.1785(7)	0.2984(9)	0.062(6)
C(23)	0.1053(13)	0.0872(8)	0.3500(9)	0.076(8)
C(24)	−0.0281(14)	0.0208(8)	0.3588(8)	0.067(7)
C(25)	−0.1474(12)	0.0452(7)	0.3122(8)	0.063(6)
C(26)	−0.1404(10)	0.1367(7)	0.2595(8)	0.054(5)
C(31)	−0.1877(10)	0.3523(6)	0.1540(6)	0.045(5)
C(32)	−0.2460(12)	0.3781(8)	0.2437(7)	0.067(6)
C(33)	−0.3845(12)	0.3975(9)	0.2299(7)	0.073(7)
C(34)	−0.4627(13)	0.3891(9)	0.1300(8)	0.072(7)
C(35)	−0.4044(12)	0.3613(9)	0.0470(8)	0.069(7)
C(36)	−0.2651(10)	0.3436(8)	0.0561(6)	0.055(5)
C(101)	0.1062(10)	0.7069(8)	0.3936(10)	0.060(6)
O	0.0635(7)	0.6378(6)	0.4696(6)	0.070(5)
C(102)	−0.0811(11)	0.6231(9)	0.4756(9)	0.072(7)
C(1)	0.2632(8)	0.7214(6)	0.3892(6)	0.037(4)
C(2)	0.3207(9)	0.6207(5)	0.3312(6)	0.036(4)
B(3)	0.3576(9)	0.6467(7)	0.4665(7)	0.035(4)
B(6)	0.3177(10)	0.7371(7)	0.2689(7)	0.040(5)
B(7)	0.4868(10)	0.6210(7)	0.3923(8)	0.042(5)
B(8)	0.5326(11)	0.7273(9)	0.4964(8)	0.050(6)
B(12)	0.5973(11)	0.7452(9)	0.3726(9)	0.054(6)
B(11)	0.4668(10)	0.6751(7)	0.2729(7)	0.042(5)
B(5)	0.3609(11)	0.8439(7)	0.3688(9)	0.052(6)
B(9)	0.5350(12)	0.8487(9)	0.4380(10)	0.058(7)
B(10)	0.4941(11)	0.8164(8)	0.2952(8)	0.048(6)
B(4)	0.3859(12)	0.7905(8)	0.4918(8)	0.048(6)
C1(1)	−0.566(3)	0.0963(18)	0.2004(19)	
C1(2)	−0.674(6)	0.054(4)	0.034(5)	
C1(3)	−0.610(8)	0.000(6)	0.056(8)	
C1(4)	−0.531(10)	−0.034(5)	−0.057(7)	
CX(1)	−0.816(13)	−0.042(8)	0.164(9)	
CX(2)	−0.884(18)	0.168(13)	−0.033(15)	

Table 4

Coordinates of refined atoms for 3

	x	y	z	U_{eq}
Au(1)	0.31219(5)	0.04654(3)	0.10622(2)	0.0493(2)
As(1)	0.40587(11)	0.22500(8)	0.06482(6)	0.0459(6)
C(11)	0.3325(11)	0.2634(8)	−0.0452(6)	0.050(6)
C(12)	0.4180(12)	0.3267(9)	−0.0871(6)	0.056(7)
C(13)	0.3575(12)	0.3616(9)	−0.1638(6)	0.058(7)
C(14)	0.2093(14)	0.3351(9)	−0.2009(6)	0.067(8)
C(15)	0.1214(12)	0.2688(11)	−0.1617(7)	0.069(8)
C(16)	0.1828(11)	0.2313(9)	−0.0835(6)	0.055(7)
C(21)	0.3455(10)	0.3624(8)	0.1166(6)	0.048(6)
C(22)	0.2629(13)	0.4520(9)	0.0727(7)	0.063(7)
C(23)	0.2158(14)	0.5438(10)	0.1172(9)	0.077(9)
C(24)	0.2561(15)	0.5435(12)	0.1972(8)	0.077(9)
C(25)	0.3360(14)	0.4576(12)	0.2383(7)	0.074(8)
C(26)	0.3850(12)	0.3654(10)	0.1986(7)	0.062(7)
C(31)	0.6260(10)	0.2347(9)	0.0857(6)	0.049(6)
C(32)	0.7063(12)	0.1340(11)	0.0755(7)	0.068(8)
C(33)	0.8640(14)	0.1410(13)	0.0857(8)	0.083(9)
C(34)	0.9416(14)	0.2434(14)	0.1102(8)	0.088(10)
C(35)	0.8605(13)	0.3418(13)	0.1198(8)	0.081(9)
C(36)	0.7039(12)	0.3381(10)	0.1086(7)	0.072(8)
C(1)	0.2266(10)	−0.1104(7)	0.1453(5)	0.042(5)

and the structures solved by Patterson syntheses (Au) and iterative full-matrix least-squares refinement/ΔF syntheses (As, C, B, O atoms) (SHELX76 [12]). Empirical absorption corrections (DIFABS [13]) were applied after isotropic convergence. Phenyl, methyl and methylene H atoms were placed in idealized positions. For **1e**, cage H atoms were positionally refined subject to a common B–H distance of 1.20(5) Å. In the final stages, all non-H atoms (except those of the solvate of **1e**) were refined with anisotropic thermal parameters, and H atoms with group isotropic parameters (cage and non-cage H atoms treated separately in the case of **1e**). The weighting scheme $w^{-1} = \sigma^2(F) + gF^2$ was applied. Details of crystal data and structure solution and refinement are given in Table 2. Atomic coordinates appear in Tables 3 and 4, respectively. Computer programs used in addition to those referenced above were CALC [14] and SHELXTL [15]. Atomic scattering factors were from *International Tables* [16] or inlaid in SHELX76. Anisotropic thermal parameters, calculated H atom positions and tables of F_o/F_c-values are available from AJW.

Molecular orbital calculations

All calculations were carried out by a locally modified version of ICON8 [17] using the weighted H_{ij} formula [18]. The model compounds AsH_3AuCH_3 (**I**) and 1-{AsH_3Au}-1,2-*closo*-$C_2B_{10}H_{11}$ (**II**) were constructed with As–H = 1.50 Å, As–Au = 2.38 Å, Au–C = 2.08 Å, C–C = C–B = B–B = 1.75 Å, B–H = $C–H_{cage}$ = 1.20 Å and $C–H_{methyl}$ = 1.08 Å, and with linear Au geometries and tetrahedral angles at C_{methyl}. The As–Au–C sequences were set to lie along the z-axis, and in **II**, C(1) was set to lie in the yz plane. H_{ii} values and orbital exponents for As, C, B and H

Table 5

Parameters [a] used in EHMO calculations

Orbital	H_{ii} (eV)	ζ_1	ζ_2	c_1	c_2
H(1*s*)	−13.30	1.30			
B(2*s*)	−15.40	1.30			
B(2*p*)	−8.68	1.30			
C(2*s*)	−20.90	1.625			
C(2*p*)	−11.10	1.625			
As(4*s*)	−16.22	2.23			
As(4*p*)	−12.16	1.89			
Au(5*d*)	−15.07	6.163	2.794	0.64418	0.53558
Au(6*s*)	−10.92	2.602			
Au(6*p*)	−5.55	2.584			

[a] Metal *d* orbitals described by double-zeta expansion.

were those inlaid in ICON8. H_{ii} values for Au were optimized for **II** at the highest level of charge iteration available, $H_{ii} = -\mathrm{VSIE}(Q)$, using nine VSIE($Q$) functions for gold (Table 5).

Results and discussion

By use of the method initially communicated by Mitchell and Stone [5], we have found that reaction between equimolar amounts of PR_3AuCl and Li[1-R'-1,2-*closo*-$C_2B_{10}H_{10}$] (prepared *in situ* from treatment of the appropriate 1,2-*closo*-carbaborane [19,20] with MeLi) in Et_2O affords the class 3 [1] phosphine gold carbaboranes 1-R'-2-PR_3Au-1,2-*closo*-$C_2B_{10}H_{10}$ (**1a–1d**, **2a–2c**) in moderate yields (for definition of individual compounds see Experimental section).

Compounds **1** and **2** are all colourless crystalline materials readily soluble in Et_2O, THF, $CHCl_3$ and CH_2Cl_2. They are indefinitely stable in the atmosphere and as the solutions prepared above. All compounds gave satisfactory microanalytical (C and H) data.

^1H NMR spectra of **1a–1d** and **2a–2c** showed resonances due to R and R' groups in the expected ratios, and confirmed the disappearance of broad peaks of integral 1 at δ 3.95 ppm (R' = CH_2OCH_3) and δ 4.00 ppm (R' = Ph) due to C*H*(2) of the parent *closo*-carbaboranes. For compounds **1a–1d**, it is of note that the resonances due to the CH_2 functions of the ether subsituent shift *ca.* 0.1 ppm to high frequency relative to that in 1-CH_2OCH_3-1,2-*closo*-$C_2B_{10}H_{11}$ [9], whilst the resonances due to the methyl part of the ether group show a smaller shift (*ca.* 0.05 ppm) in the opposite direction. ^{31}P-{^1H} NMR spectra of **1a–1d** and **2a–2c** all show the expected singlet resonances, the chemical shifts of which were found to lie between 1 and 8 ppm to higher frequency than those of the appropriate PR_3AuCl species and between 6 and 28 ppm to lower frequency of those of the appropriate PR_3AuCH_3 species [1,21]. ^{11}B-{^1H} NMR spectra of the gold carbaboranes all show two peaks of integral 1 at highest frequency [B(9) and B(12)] but, at the field strength used, the spectra do not totally distinguish between the four pairs of low frequency symmetry-equivalent boron atoms, compounds **1** displaying a triple coincidence at lowest frequency and compounds **2** two double coincidences. ^{11}B spectra show that all signals experience doublet coupling, with ^1J(BH)

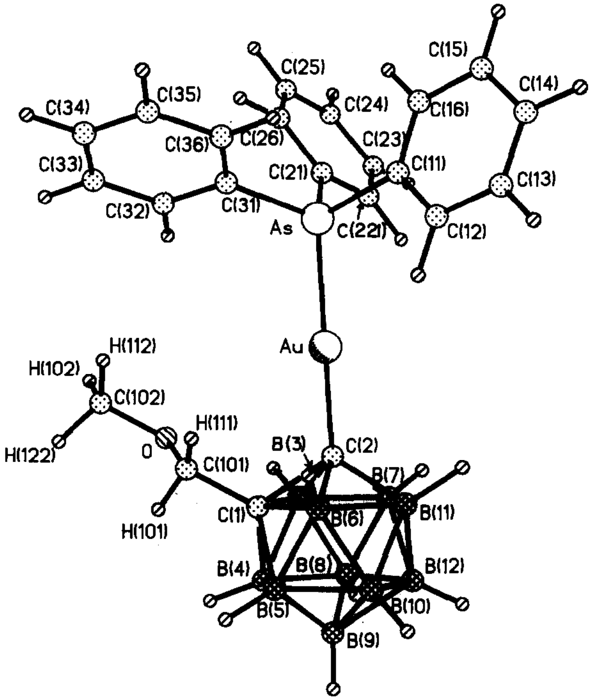

Fig. 1. Perspective view of compound 1e. Cage H atoms carry the same number as the B to which they are bound.

in the range 140–176 Hz. In $1\text{-}CH_2OCH_3\text{-}1,2\text{-}closo\text{-}C_2B_{10}H_{11}$, the range of ^{11}B chemical shifts in $CDCl_3$ is −2.47 to −12.45 ppm [9], and in 1-Ph-1,2-*closo*-$C_2B_{10}H_{11}$, it is −1.30 to −12.01 ppm [4]. Clearly, when H(2) in these carbaboranes is replaced by a $\{PR_3Au\}$ moiety all ^{11}B chemical shifts move to high frequency, especially those least far from the carbaborane cage carbon atoms. This suggests that the carbaborane cages in **1** and **2** could be functioning as moderately efficient electron donors to the metal fragment (*vide infra*).

The $AsPh_3$ derivatives **1e** and **2e** were prepared similarly from $AsPh_3AuCl$ and were characterized by microanalysis and ^1H and ^{11}B NMR spectroscopies. The $AsPh_3$ ligand in **1e** (and presumably also in **2e**) is easily replaced by PPh_3 to afford **1a** (**2a**) as identified by $^{31}P\text{-}\{^1H\}$ NMR spectroscopy.

Both **1a** and **1e** afford high quality crystals from CH_2Cl_2/hexane (1:4), and these were shown to be isomorphous by unit cell determinations. However, crystals of **1a** became opaque after *ca.* 20 h at room temperature, presumably through solvate loss, so intensity data were collected from **1e** at low temperature.

Figure 1 shows a perspective view of a single molecule of **1e** and demonstrates the atomic numbering scheme used; Table 6 details interatomic distances and interbond angles determined. Compound **1e** co-crystallizes with one molecule of CH_2Cl_2 solvate but the latter is disordered in the lattice and relatively poorly defined. In **1e**, the $\{1,2\text{-}closo\text{-}C_2B_{10}\}$ cage has the expected icosahedral geometry, with C(1)–C(2) = 1.667(11) Å, longer (although not significantly so) than that in the parent species $1\text{-}CH_2OCH_3\text{-}1,2\text{-}closo\text{-}C_2B_{10}H_{11}$ [9]. The phenyl rings adopt a

Table 6

Interatomic distances (Å) and interbond angles (deg) in **1e**

Au–As	2.3740(8)	C(1)–B(6)	1.698(12)
Au–C(2)	2.039(8)	C(1)–B(5)	1.695(13)
As–C(11)	1.943(8)	C(1)–B(4)	1.705(13)
As–C(21)	1.922(8)	C(2)–B(3)	1.717(11)
As–C(31)	1.933(8)	C(2)–B(6)	1.730(12)
C(11)–C(12)	1.389(13)	C(2)–B(7)	1.693(12)
C(11)–C(16)	1.354(13)	C(2)–B(11)	1.716(12)
C(12)–C(13)	1.373(14)	B(3)–B(7)	1.732(13)
C(13)–C(14)	1.360(15)	B(3)–B(8)	1.760(14)
C(14)–C(15)	1.429(16)	B(3)–B(4)	1.789(13)
C(15)–C(16)	1.369(15)	B(6)–B(11)	1.781(13)
C(21)–C(22)	1.367(13)	B(6)–B(5)	1.744(14)
C(21)–C(26)	1.369(12)	B(6)–B(10)	1.764(14)
C(22)–C(23)	1.366(16)	B(7)–B(8)	1.776(14)
C(23)–C(24)	1.405(16)	B(7)–B(12)	1.760(15)
C(24)–C(25)	1.336(15)	B(7)–B(11)	1.720(13)
C(25)–C(26)	1.375(14)	B(8)–B(12)	1.785(15)
C(31)–C(32)	1.391(13)	B(8)–B(9)	1.755(16)
C(31)–C(36)	1.359(12)	B(8)–B(4)	1.769(15)
C(32)–C(33)	1.404(15)	B(12)–B(11)	1.724(14)
C(33)–C(34)	1.385(16)	B(12)–B(9)	1.764(16)
C(34)–C(35)	1.325(16)	B(12)–B(10)	1.745(15)
C(35)–C(36)	1.404(14)	B(11)–B(10)	1.757(14)
C(101)–O	1.394(13)	B(5)–B(9)	1.786(16)
C(101)–C(1)	1.498(13)	B(5)–B(10)	1.766(15)
O–C(102)	1.384(14)	B(5)–B(4)	1.762(15)
C(1)–C(2)	1.667(11)	B(9)–B(10)	1.820(16)
C(1)–B(3)	1.725(11)	B(9)–B(4)	1.721(16)

As–Au–C(2)	177.05(21)	B(7)–C(2)–B(11)	60.6(5)
Au–As–C(11)	113.51(24)	C(1)–B(3)–C(2)	58.0(4)
Au–As–C(21)	113.87(23)	C(1)–B(3)–B(4)	58.0(5)
Au–As–C(31)	113.61(25)	C(2)–B(3)–B(7)	58.8(5)
C(11)–As–C(21)	104.4(3)	B(7)–B(3)–B(8)	61.1(5)
C(11)–As–C(31)	105.6(3)	B(8)–B(3)–B(4)	59.8(6)
C(21)–As–C(31)	103.8(3)	C(1)–B(4)–C(2)	58.2(5)
As–C(11)–C(12)	117.7(6)	C(1)–B(6)–B(5)	59.0(5)
As–C(11)–C(16)	121.3(7)	C(2)–B(6)–B(11)	58.5(5)
C(12)–C(11)–C(16)	121.0(8)	B(11)–B(6)–B(10)	59.4(5)
C(11)–C(12)–C(13)	119.3(9)	B(5)–B(6)–B(10)	60.5(6)
C(12)–C(13)–C(14)	121.0(10)	C(2)–B(7)–B(3)	60.2(5)
C(13)–C(14)–C(15)	119.0(10)	C(2)–B(7)–B(11)	60.4(5)
C(14)–C(15)–C(16)	119.3(10)	B(3)–B(7)–B(8)	60.2(5)
C(11)–C(16)–C(15)	120.4(10)	B(8)–B(7)–B(12)	60.7(6)
As–C(21)–C(22)	118.1(6)	B(12)–B(7)–B(11)	59.4(6)
As–C(21)–C(26)	122.8(6)	B(3)–B(8)–B(7)	58.6(5)
C(22)–C(21)–C(26)	119.2(8)	B(3)–B(8)–B(4)	60.9(6)
C(21)–C(22)–C(23)	120.3(9)	B(7)–B(8)–B(12)	59.2(6)
C(22)–C(23)–C(24)	119.8(10)	B(12)–B(8)–B(9)	59.8(6)
C(23)–C(24)–C(25)	119.4(10)	B(9)–B(8)–B(4)	58.5(6)
C(24)–C(25)–C(26)	120.4(10)	B(7)–B(12)–B(8)	60.1(6)
C(21)–C(26)–C(25)	120.9(9)	B(7)–B(12)–B(11)	59.2(6)
As–C(31)–C(32)	116.6(7)	B(8)–B(12)–B(9)	59.3(6)
As–C(31)–C(36)	123.0(7)	B(11)–B(12)–B(10)	60.8(6)
C(32)–C(31)–C(36)	120.4(8)	B(9)–B(12)–B(10)	62.5(6)

Table 6 (continued)

C(31)–C(32)–C(33)	118.2(9)	C(2)–B(11)–B(6)	59.2(5)
C(32)–C(33)–C(34)	121.2(10)	C(2)–B(11)–B(7)	59.0(5)
C(33)–C(34)–C(35)	118.5(11)	B(6)–B(11)–B(10)	59.8(5)
C(34)–C(35)–C(36)	122.6(10)	B(7)–B(11)–B(12)	61.5(6)
C(31)–C(36)–C(35)	119.0(9)	B(12)–B(11)–B(10)	60.2(6)
O–C(101)–C(1)	110.9(8)	C(1)–B(5)–B(6)	59.2(5)
C(101)–O–C(102)	112.2(8)	C(1)–B(5)–B(4)	59.1(5)
C(101)–C(1)–C(2)	118.6(7)	B(6)–B(5)–B(10)	60.3(6)
C(101)–C(1)–B(3)	118.4(7)	B(9)–B(5)–B(10)	61.6(6)
C(101)–C(1)–B(6)	117.1(7)	B(9)–B(5)–B(4)	58.0(6)
C(101)–C(1)–B(5)	119.7(7)	B(8)–B(9)–B(12)	61.0(6)
C(101)–C(1)–B(4)	120.6(7)	B(8)–B(9)–B(4)	61.2(6)
B(3)–C(1)–C(2)	60.8(5)	B(12)–B(9)–B(10)	58.3(6)
B(3)–C(1)–B(4)	62.9(5)	B(5)–B(9)–B(10)	58.7(6)
B(6)–C(1)–C(2)	61.9(5)	B(5)–B(9)–B(4)	60.3(6)
B(6)–C(1)–B(5)	61.9(5)	B(6)–B(10)–B(11)	60.8(5)
B(5)–C(1)–B(4)	62.4(6)	B(6)–B(10)–B(5)	59.2(6)
Au–C(2)–C(1)	119.3(5)	B(12)–B(10)–B(11)	59.0(6)
Au–C(2)–B(3)	120.4(5)	B(12)–B(10)–B(9)	59.3(6)
Au–C(2)–B(6)	116.0(5)	B(5)–B(10)–B(9)	59.7(6)
Au–C(2)–B(7)	124.1(5)	C(1)–B(4)–B(3)	59.1(5)
Au–C(2)–B(11)	121.5(5)	C(1)–B(4)–B(5)	58.5(5)
B(3)–C(2)–C(1)	61.3(5)	B(3)–B(4)–B(8)	59.3(5)
B(3)–C(2)–B(7)	61.1(5)	B(8)–B(4)–B(9)	60.4(6)
B(6)–C(2)–C(1)	59.9(5)	B(5)–B(4)–B(9)	61.7(6)
B(6)–C(2)–B(11)	62.3(5)		

propellar-like arrangement at the As atom with twist angles about the As–C(11), As–C(21) and As–C(31) bonds of 24, 43 and 60°, respectively, where 0° twist corresponds to an eclipsed Au–As–C–C arrangement. The orientation of the ether substituent is defined by the C(2)–C(1)–C(101)–O torsion angle of 74.9° and the C(1)–C(101)–O–C(102) torsion angle of 179.8° (*trans* staggered), and results in the closest interligand contact being between H(112) and H(32), 2.66 Å. The O...Au distance is 3.582(7) Å, too long to suggest interaction. In the related, isoelectronic compound, $1\text{-CH}_2\text{OC}_2\text{H}_5\text{-2-(CH}_3\text{Hg)-1,2-}closo\text{-C}_2\text{B}_{10}\text{H}_{10}$ [22], the C(2)–C(1)–C–O torsion angle is close to 0°, and Hg...O is only 2.747(4) Å, both of which imply some degree of secondary bonding between the ether oxygen atom and the metal.

The As–Au–C(2) sequence is essentially linear and Au–As = 2.3740(8) Å, Au–C(2) = 2.039(8) Å. There are no published $\text{Au–C}_{\text{carbaborane}}$ σ-bonded distances against which to compare the latter value, but a single bond Au–C distance *trans* to AsPh_3 could be expected to be *ca.* 2.1 Å by consideration of the Au–CH_3 and Au–Br bond lengths of 2.123 and 2.407 Å in PPh_3AuMe [23] and PPh_3AuBr [24], respectively ($\Delta = 0.28$ Å) together with the Au–Br bond length of 2.37 Å in AsPh_3AuBr [25]. On this basis, the Au–C(2) bond length in **1e** appears to be unusually short. However, it was clearly of importance to determine the length of an Au–C single bond *trans* to AsPh_3 in a standard compound before further consideration was given to the above result, and to this end, we have synthesized AsPh_3AuMe (**3**) by established methods [10] and determined its molecular structure.

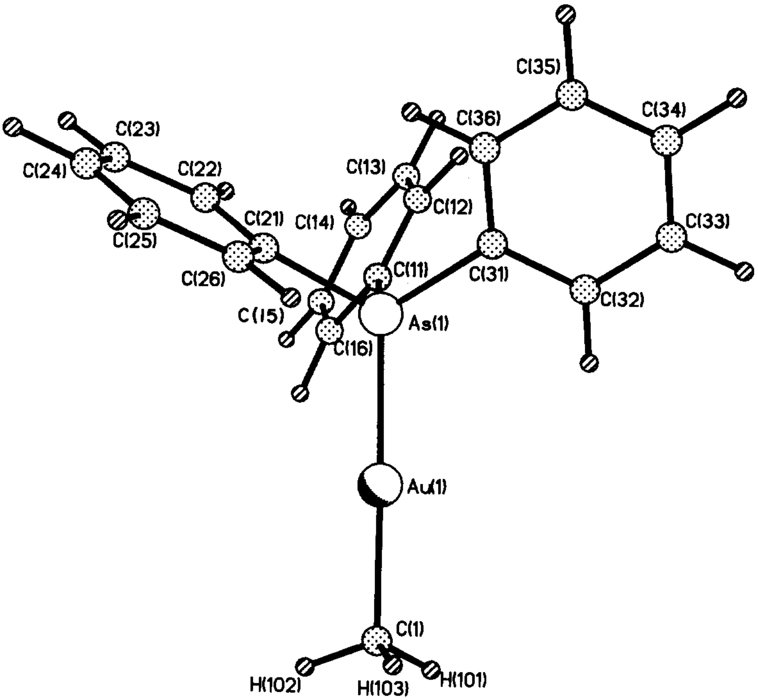

Fig. 2. Perspective view of compound 3.

Figure 2 shows a perspective view of a single molecule of **3** and Table 7 lists interatomic distances and interbond angles determined. In **3**, the disposition of the phenyl rings is again propellar-like, with twist angles of 32, 57 and 37° about the As–C(11), As–C(21) and As–C(31) bonds, respectively. The Au–As distance is within 0.0060(14) Å of that of **1e**, but the Au–C distance in **3** is 0.085(12) Å longer than in the carbaborane compound, supporting the proposal that in **1e** the Au–C sigma bond is anomalously short.

The origin of this unexpected result was investigated by analysis of the results of extended Hückel molecular orbital (EHMO) calculations on the model compounds **I** and **II** (Table 8). Comparison of the reduced overlap population matrix (ROPM) elements confirms that the Au–As bond strengths in **I** and **II** are essentially the same, and shows that the shorter Au–C distance in **1e** relative to that in **3** is due to increased bond strength in the former compound. In **II**, the gold atom carries a greater negative charge ($\Delta = 0.018$ e), and analysis of the individual atomic orbital occupations (AOOs) shows that this increased charge lies predominantly in the $6p_z$ and $6s$ AOs.

Taken together, these results imply that the carbaborane ligand of **1e** is a *better σ-donor* than the methyl ligand of **3**. Calculations on $[CH_3]^-$ and $[1,2\text{-}closo\text{-}C_2B_{10}H_{11}]^-$ (the latter derived from **II** by removal of the $\{H_3AsAu\}^+$ fragment) confirm that this is reasonable since the highest occupied MO (HOMO) of the carbaborane ligand lies *ca.* 1 eV higher than that of $[CH_3]^-$ (−10.676 *vs.* −11.749 eV, respectively). This results from the fact that, whilst the HOMO of $[CH_3]^-$ is the expected carbon ($2s$–$2p_z$) hybrid orbital directed towards the 4th tetrahedral

Table 7

Interatomic distances (Å) and interbond angles (deg) in **3**

Au(1)-As(1)	2.3800(11)	C(21)-C(26)	1.382(15)
Au(1)-C(1)	2.124(9)	C(22)-C(23)	1.426(17)
As(1)-C(11)	1.913(10)	C(23)-C(24)	1.349(19)
As(1)-C(21)	1.949(10)	C(24)-C(25)	1.314(19)
As(1)-C(31)	1.929(10)	C(25)-C(26)	1.389(17)
C(11)-C(12)	1.389(14)	C(31)-C(32)	1.390(15)
C(11)-C(16)	1.396(14)	C(31)-C(36)	1.376(15)
C(12)-C(13)	1.368(15)	C(32)-C(33)	1.390(18)
C(13)-C(14)	1.364(16)	C(33)-C(34)	1.372(20)
C(14)-C(15)	1.392(17)	C(34)-C(35)	1.370(20)
C(15)-C(16)	1.402(16)	C(35)-C(36)	1.376(18)
C(21)-C(22)	1.376(15)		
As(1)-Au(1)-C(1)	178.60(24)	As(1)-C(21)-C(26)	117.9(8)
Au(1)-As(1)-C(11)	116.0(3)	C(22)-C(21)-C(26)	121.2(10)
Au(1)-As(1)-C(21)	112.5(3)	C(21)-C(22)-C(23)	115.8(10)
Au(1)-As(1)-C(31)	114.7(3)	C(22)-C(23)-C(24)	121.3(12)
C(11)-As(1)-C(21)	102.3(4)	C(23)-C(24)-C(25)	122.2(13)
C(11)-As(1)-C(31)	104.8(4)	C(24)-C(25)-C(26)	119.4(12)
C(21)-As(1)-C(31)	105.1(4)	C(21)-C(26)-C(25)	120.1(10)
As(1)-C(11)-C(12)	123.2(8)	As(1)-C(31)-C(32)	118.2(8)
As(1)-C(11)-C(16)	117.9(7)	As(1)-C(31)-C(36)	122.0(8)
C(12)-C(11)-C(16)	118.9(9)	C(32)-C(31)-C(36)	119.8(10)
C(11)-C(12)-C(13)	121.7(10)	C(31)-C(32)-C(33)	119.1(11)
C(12)-C(13)-C(14)	120.1(10)	C(32)-C(33)-C(34)	120.9(13)
C(13)-C(14)-C(15)	119.9(11)	C(33)-C(34)-C(35)	119.1(13)
C(14)-C(15)-C(16)	120.5(11)	C(34)-C(35)-C(36)	121.1(12)
C(11)-C(16)-C(15)	118.9(10)	C(31)-C(36)-C(35)	119.9(11)
As(1)-C(21)-C(22)	120.9(8)		

Table 8

Summary of pertinent results from EHMO calculations on **I** and **II**

	I	**II**	**Δ (II–I)**
ROPM elements			
Au–As	0.6296	0.6310	0.0014
Au–C	0.5323	0.5797	0.0474
Net atomic charge (e)			
Au	0.0009	−0.0173	−0.0182
Gold AOO (e)			
$6s$	0.8127	0.8197	0.0070
$6p_x$	0.0015	0.0065	0.0050
$6p_y$	0.0015	0.0040	0.0025
$6p_z$	0.3488	0.3638	0.0150
$5d_{x^2-y^2}$	1.9999	1.9998	−0.0001
$5d_{z^2}$	1.8619	1.8607	−0.0012
$5d_{xy}$	1.9999	1.9998	−0.0001
$5d_{xz}$	1.9865	1.9828	−0.0037
$5d_{yz}$	1.9865	1.9802	−0.0063

position, that of $[1,2\text{-}closo\text{-}C_2B_{10}H_{11}]^-$, although localized mainly on C(2) (30%) and outpointing from the *closo* icosahedron, has substantial boron character (total of 60%, divided more or less equally between 7 boron atoms).

Conclusions

This study has demonstrated that the stability of the gold-carbaborane σ-bond in class 3 phosphine and arsine gold carbaborane compounds is primarily due to the carbaborane acting as an efficient σ-donor, in contrast to previous (and indeed current [26]) descriptions of its ligand function. In turn, this suggests that stable class 3 carbametallaboranes could be formed with high oxidation state, low d^n configuration metal centres. Future contributions will report the results of studies stimulated by these conclusions.

Note added in proof

Since submission of this paper we have become aware that the related compound $1\text{-}Ph_3PAu\text{-}1,2\text{-}closo\text{-}C_2B_{10}H_{11}$ has been structurally characterized (T.V. Baukova *et al.*, Metallogr. Khim., 2 (1989) 1098). In this Au–C is 2.039(8) Å, exactly the same as in the **1e**. This bond length is 0.085 Å shorter than that in Ph_3PAuMe [23], thus corroborating the conclusions reached in our studies.

Acknowledgments

We thank the SERC for support (BDR), Johnson Matthey plc for a loan of gold salts and the Callery Chemical Company for a generous gift of decaborane.

References

1 A.J. Wynd, A.J. McLennan, D. Reed and A.J. Welch, J. Chem. Soc., Dalton Trans., (1987) 2761.
2 S. Bresodola, in R.N. Grimes (Ed.), Metal Interactions with Boron Clusters, Plenum, New York, 1982.
3 D.A. Owen, J.C. Smart, P.M. Garrett and M.F. Hawthorne, J. Am. Chem. Soc., 93 (1971) 1362.
4 B.D. Reid, Ph.D. Thesis, University of Edinburgh, 1992.
5 C.M. Mitchell and F.G.A. Stone, J. Chem. Soc., Chem. Commun., (1970) 1263.
6 D.G. Evans and D.M.P. Mingos, J. Organometal. Chem., 232 (1982) 171.
7 M.I. Bruce, B.K. Nicholson and O. Bin Shawkataly, Inorg. Synth., 26 (1989) 324.
8 T.L. Heying, J.W. Ager, Jr., S.L. Clark, D.J. Mangold, R.L. Goldstein, M. Hillman, R.J. Polak and J.W. Szymanski, Inorg. Chem., 2 (1963) 1089.
9 K.F. Shaw and A.J. Welch, Polyhedron, 11 (1992) 157.
10 H. Schmidbaur, T. Pollock, R. Herr, F.E. Wagner, R. Bau, J. Riede and G. Muller, Organometallics, 5 (1986) 566.
11 R.O. Gould and D.E. Smith, CADABS, University of Edinburgh, 1986.
12 G.M. Sheldrick, SHELX76, University of Cambridge, 1976.
13 N.G. Walker and D. Stuart, Acta Crystallogr., Sect. A, 39 (1983) 158.
14 R.O. Gould and P. Taylor, CALC, University of Edinburgh, 1986.
15 G.M. Sheldrick, SHELXTL, University of Göttingen, 1985.
16 International Tables for X-Ray Crystallography, Kynoch Press, Birmingham, Vol. 4, 1974, p. 99.
17 J. Howell, A. Rossi, D. Wallace, K. Haraki and R. Hoffmann, ICON8, Quantum Chemistry Program Exchange, University of Indiana, no. 344.
18 J.H. Ammeter, H.-B. Burgi, J.C. Thibeault and R. Hoffmann, J. Am. Chem. Soc., 100 (1982) 3686.

19 M.A. Bennett and P.A. Longstaff, Chem. Ind. (London), (1965) 846.
20 P.M. Garrett, J.C. Smart and M.F. Hawthorne, J. Am. Chem. Soc., 91 (1969) 4707.
21 A.J. Wynd, Ph.D. Thesis, University of Edinburgh, 1988.
22 A.I. Yanovskii, Yu.T. Struchkov, V.N. Kalinin, O.M. Zurlova and L.I. Zakharkin, Zh. Struct. Khim., 22 (1981) 120.
23 P.D. Gavens, J.J. Guy, J.J. Mays and G.M. Sheldrick, Acta Crystallogr., Sect. B, 33 (1977) 137.
24 P.F. Barron, L.M. Englehardt, P.C. Healy, J. Oddy and A.H. White, Aust. J. Chem., 40 (1987) 1545.
25 F.W.B. Einstein and R. Restivo, Acta Crystallogr., Sect. B, 31 (1975) 624.
26 X. Yang, C.B. Knobler and M.F. Hawthorne, Angew. Chem. Int. Ed. Engl., 30 (1991) 1507.